




Invariance property in inhomogeneous scattering media with refractive-index mismatchFederico Tommasi ,* Lorenzo Fini , Fabrizio Martelli , and Stefano Cavalieri*Dipartimento di Fisica e Astronomia, Università di Firenze, Via Giovanni Sansone 1 I-50019 Sesto Fiorentino, Italy*

(Received 14 May 2020; accepted 2 September 2020; published 6 October 2020)

The mean path-length invariance property is a very important property of scattering media illuminated by an isotropic and homogeneous radiation. Here, we investigate the case of inhomogeneous media with refractive-index mismatch between the external environment and also among their subdomains. The invariance property remains valid by the introduction of a correction, dependent on the refractive index, of the mean path-length value. It is a consequence of the stationary solution of the radiative transfer equation in a medium subjected to an isotropic and homogeneous radiance. The theoretical results are in agreement with the reported results for numerical simulations for both the three-dimensional and the two-dimensional media.

DOI: [10.1103/PhysRevA.102.043501](https://doi.org/10.1103/PhysRevA.102.043501)**I. INTRODUCTION**

Light scattering in optical media is a research field that involves a wide range of different theoretical and experimental issues, such as light propagation in biological tissue [1–4], random lasers [5–9], Anderson localization [10,11], anomalous diffusion [12–14], and replica symmetry breaking phenomena [15–17]. Moreover, concerning the applications, light diffusion has also been studied in optical sensing [18–22] and to find new design for solar cells in order to enhance the absorption effects [23–27]; in this regard, it has been reported that a small amount of scattering can promote the absorption in a thin slab subjected to monodirectional illumination [28].

A fascinating and also, at first glance, counterintuitive invariance property holds for the mean total path-length $\langle L \rangle$ spent by light propagating inside a disordered medium, and, in general, also by any kind of particle under diffusion and random walk. Under the hypothesis of isotropic and uniform illumination upon the surface of the medium, $\langle L \rangle$ only depends on the geometry of the medium, whatever is its scattering strength, usually described by the scattering coefficient μ_s . Such an invariance property (IP) [29–31], also known as a Cauchy formula, is a generalization, in the case of scattering of the mean chord theorem, also described by Dirac in the context of nuclear physics [32]. Recently, the experimental observation of the IP has been reported in the optical case [33] and in the context of biology by studying the random walks of bacteria in a complex structure [34].

The IP remains valid also considering bounded domains of different dimensions; in the three-dimensional (3D) and in the two-dimensional (2D) case, $\langle L \rangle$ is proportional to the volume-surface ratio and the surface-perimeter ratio, respectively,

$$\langle L \rangle_{3D} = 4 \frac{V}{S}, \quad (1)$$

$$\langle L \rangle_{2D} = \pi \frac{S}{P}. \quad (2)$$

Geometrical details and strength of the disorder do not play any role in determining the value of $\langle L \rangle$. Moreover, generalizations of the IP property have been reported in the case of inhomogeneous random media [35], stochastic mixture media [36], and in the presence of absorption and branching [37,38].

Here, we consider the usual case where the scattering process can be described by the radiative transfer equation (RTE).

The IP remains valid also in case of a infinitely extending medium, such as a thin slab, and with different values of the asymmetry factor g of the scattering function [28].

In this paper, we investigate how such property with suitable modifications still holds in the case of refractive-index mismatch between the disordered medium and the external environment. We have investigated the case of inhomogeneous media with refractive-index mismatch between the external environment and among their subdomains, both in 3D and in 2D geometry.

II. THEORY

In this paper, we have studied media where scattering plays the leading role and, then, where interference effects due to refractive-index mismatches are destroyed or strongly reduced. Our analytical and numerical results are, indeed, valid in such a condition. Interference effects due to the bulk structure should be considered near the condition of Anderson localization, i.e., $\mu_s \lambda = \lambda / l_s \approx 1$, where l_s is the scattering mean free path. However, our simulation, and analytical results, are, indeed, conceived for the optical or near-infrared spectral region where $l_s / \lambda \gg 1$.

To express the boundary condition between two scattering media 1 and 2, one has to take into account that light intensity can be transferred reciprocally between the media (see Fig. 1). The physical condition is that the power flowing in the generic direction \hat{s}_2 per unit of time and surface at \vec{r} on the boundary Σ must be equal to the sum of the fraction of the transmitted power per unit of time and surface (from medium 1 to medium 2) around the direction \hat{s}_1 and the fraction of the reflected power per unit of time and surface around the outgoing

*federico.tommasi@unifi.it

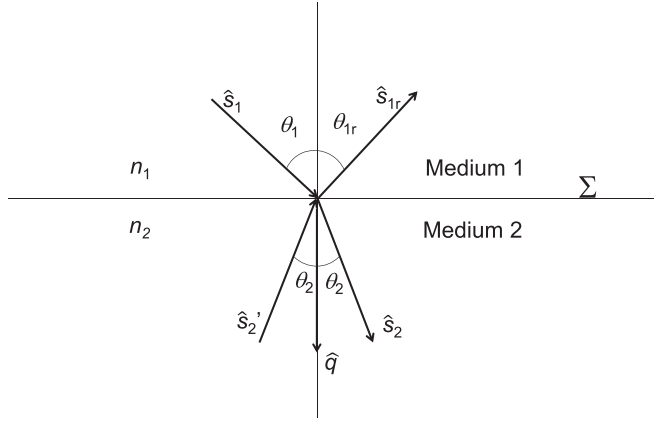


FIG. 1. Schematic of a plane boundary between two media (2D section) and used symbols: n_1 and n_2 are the refractive indices of medium 1 and medium 2, and q is the normal direction to the boundary and Σ the interface boundary.

direction \hat{s}'_2 where the directions \hat{s}_2 and \hat{s}_1 are related by Snell's law, whereas \hat{s}'_2 is the mirror image direction of \hat{s}_2 (with respect to Σ).

The relation can be written in full generality in terms of radiance (power per unit of time, surface, and solid angle) $I_2(\vec{r}, \hat{s}_2, t)$, $I_2(\vec{r}, \hat{s}'_2, t)$, and $I_1(\vec{r}, \hat{s}_1, t)$ for any point \vec{r} belonging to Σ and for any incoming direction s_2 from medium 1 to medium 2 as

$$\begin{aligned} I_2(\vec{r}, \hat{s}_2, t) \cos \theta_2 d\Omega_2 \\ = [1 - R_{F12}(\theta_1)] I_1(\vec{r}, \hat{s}_1, t) \cos \theta_1 d\Omega_1 \\ + R_{F21}(\theta_2) I_2(\vec{r}, \hat{s}'_2, t) \cos \theta_2 d\Omega_2, \end{aligned} \quad (3)$$

with $\theta_2 = \arcsin(\frac{n_1}{n_2} \sin \theta_1)$, R_{F12} reflection coefficient for the transfer from medium 1 to medium 2 for nonpolarized radiation, and R_{F21} reflection coefficient for the transfer from medium 2 to medium 1 and with $d\Omega_1$ and $d\Omega_2$ infinitesimal solid angles around the directions \hat{s}_1 and \hat{s}_2 , respectively. Then, taking into account Snell's law (and its differential) one obtains

$$\begin{aligned} I_2(\vec{r}, \hat{s}_2, t) - R_{F21}(\theta_2) I_2(\vec{r}, \hat{s}'_2, t) \\ = [1 - R_{F12}(\theta_1)] I_1(\vec{r}, \hat{s}_1, t) \left(\frac{n_2}{n_1}\right)^2. \end{aligned} \quad (4)$$

It is worth noting that $R_{F21}(\theta_2) = R_{F12}(\theta_1)$ for all the incoming directions for which a refracted beam exists [39].

The procedure can be applied also to a 2D geometry where the radiance is defined as the power per unit of time, length, and angle, resulting in

$$\begin{aligned} I_2(\vec{r}, \hat{s}_2, t) \cos \theta_2 d\theta_2 = [1 - R_{F12}(\theta_1)] I_1(\vec{r}, \hat{s}_1, t) \cos \theta_1 d\theta_1 \\ + R_{F21}(\theta_2) I_2(\vec{r}, \hat{s}'_2, t) \cos \theta_2 d\theta_2. \end{aligned} \quad (5)$$

Proceeding similarly to the previous case, one obtains the 2D result,

$$\begin{aligned} I_2(\vec{r}, \hat{s}_2, t) - R_{F21}(\theta_2) I_2(\vec{r}, \hat{s}'_2, t) \\ = [1 - R_{F12}(\theta_1)] I_1(\vec{r}, \hat{s}_1, t) \left(\frac{n_2}{n_1}\right). \end{aligned} \quad (6)$$

A. Boundary of a nonabsorbing medium subjected to Lambertian illumination

The case of the continuous wave Lambertian illumination is a significant case where the boundary conditions assume a particularly simple form, and it is the main hypothesis of the invariance property in presence of scattering. Let it be a uniform isotropic illumination applied at the external boundary Σ of a finite, uniform, scattering and nonabsorbing medium of volume V : $I_1(\vec{r}, \hat{s}_1, t) = I_1$ for $\forall \vec{r} \in \Sigma$. For such a condition, it can be verified that at the interior of the volume a homogeneous and isotropic radiance of the form

$$I_2(\vec{r}, \hat{s}_2) = I_2 = I_1 \left(\frac{n_2}{n_1}\right)^2 \quad (7)$$

is a stationary solution of the RTE equation and satisfies the boundary conditions of Eq. (4) with $R_{F21}(\theta_2) = R_{F12}(\theta_1)$.

The analog result of Eq. (7) is obtained in 2D,

$$I_2(\vec{r}, \hat{s}_2) = I_2 = I_1 \left(\frac{n_2}{n_1}\right). \quad (8)$$

For a more general case, let us now assume that the volume V is inhomogeneous in scattering with several discrete subvolumes V_i . Once the incoming radiance I_1 is uniformly and isotropically incident on the surface Σ containing the total volume (hypothesis of the invariance property), the solution of the RTE in any volume is again a uniform radiance I_i in any subvolumes V_i . For such a solution, the connection of the radiances between adjacent volumes V_i and V_j will be then equal to that of Eqs. (7) and (8), that is as follows:

$$I_j = I_i \left(\frac{n_j}{n_i}\right)^2, \quad (9)$$

in 3D and

$$I_j = I_i \left(\frac{n_j}{n_i}\right), \quad (10)$$

in 2D.

With reference to Figs. 2 and 3, it is interesting to note that the radiance in any subvolume can be expressed by means of the radiance I_1 incoming on the more external surface Σ , the external index of refraction n_1 and the refraction index n_i of the specific subvolume,

$$I_i = I_1 \left(\frac{n_i}{n_1}\right)^2, \quad (11)$$

in 3D and

$$I_i = I_1 \left(\frac{n_i}{n_1}\right), \quad (12)$$

in 2D.

B. Invariance property: inhomogeneous case for the refractive index

Equations (1) and (2) can be generalized to the case of media with inhomogeneous refractive index. Let us assume to have an inhomogeneous medium, such as described in the previous section. Following the approach of Blanco and Fournier [29], we assume to have a very small absorption coefficient μ_a throughout the volume, and we equate the power absorbed

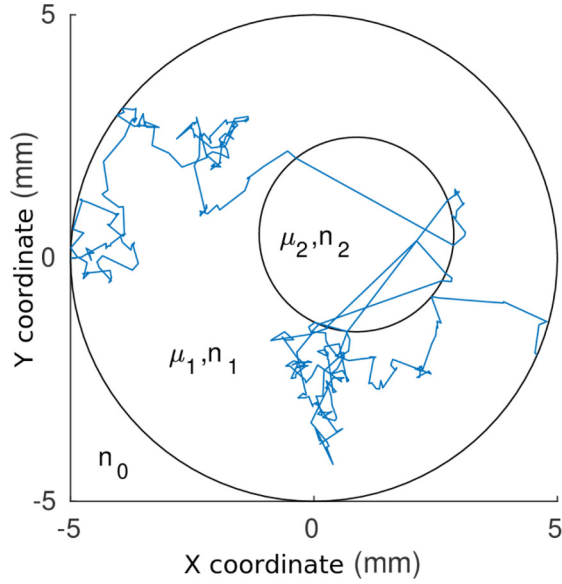


FIG. 2. Example of trajectory in the MC simulation of a 2D random walk inside a bounded circular domain with a circular decentered inhomogeneity. The starting position is located in the boundary of the larger medium at coordinates $(-5, 0)$ mm. The refractive index n_0 of the external environment is 1. The largest medium has refractive index $n_1 = 2$ and scattering coefficient $\mu_1 = 5 \text{ mm}^{-1}$, whereas in the inhomogeneity $n_2 = 1$ and $\mu_2 = 0.1 \text{ mm}^{-1}$.

in volume V to the absorption of the power impinging the external surface from outside (let us label with “ e ” the quantity referred to the outside).

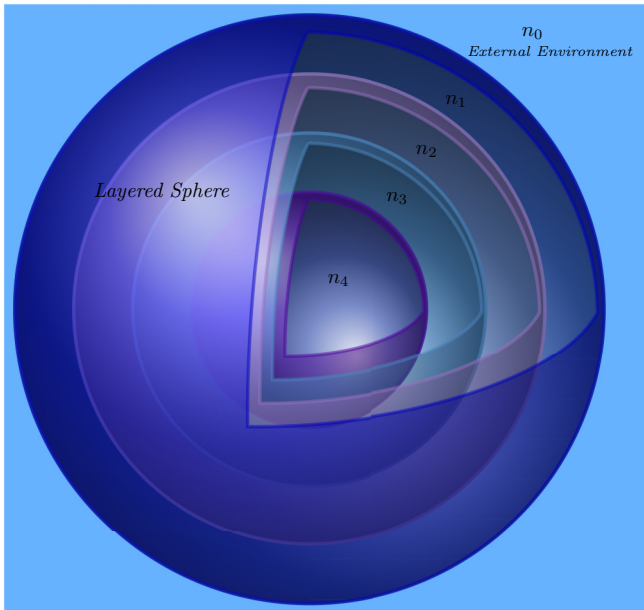


FIG. 3. Structure of the layered sphere, with the refractive index and the scattering coefficient of each layer. The radiation impinges, from the external environment to the surface of the outermost layer, in the Lambertian way.

For the last quantity, assuming μ_a is constant in all volumes, in the limit $\mu_a \rightarrow 0$, we have as follows:

$$P_A = \pi S I_e \int_0^{+\infty} [1 - \exp(-\mu_a L)] P(L) dL = \pi S I_e \mu_a \langle L \rangle, \quad (13)$$

where $P(L)$ is the probability density function to have a path-length L within the whole volume V when a Lambertian illumination is impinging on the external boundary Σ of area S .

As stated above, the power absorbed is also given by the absorption in the volume,

$$P_A = \mu_a \int_V d\vec{r} \int_{4\pi} I(\vec{r}, \hat{s}) d\hat{s} = \mu_a \sum_{i=1}^N \int_{V_i} d\vec{r} \int_{4\pi} I_i(\vec{r}, \hat{s}) d\hat{s}. \quad (14)$$

Using the expression of the radiance obtained in the previous section, we have as follows:

$$P_A = \mu_a \sum_{i=1}^N \int_{V_i} d\vec{r} \int_{4\pi} I_i(\vec{r}, \hat{s}) d\hat{s} = 4\pi I_e \sum_{i=1}^N V_i \left(\frac{n_i}{n_e} \right)^2, \quad (15)$$

and, then,

$$\langle L \rangle = 4 \frac{\sum_{i=1}^N V_i \left(\frac{n_i}{n_e} \right)^2}{S}. \quad (16)$$

Such an equation has been heuristically used in the paper of Savo *et al.* [33] limited to the case of homogeneous medium ($N = 1$).

In the case of 2D geometry, we follow a similar approach. We equal the power absorbed in the surface S to the absorption of the power impinging the perimeter P from outside. The latter in the limit $\mu_a \rightarrow 0$ is given by

$$P_A = 2\pi I_e \int_0^{+\infty} [1 - \exp(-\mu_a L)] p_L(L) dL = 2\pi I_e \mu_a \langle L \rangle, \quad (17)$$

whereas the power absorbed in the surface S is as follows:

$$P_A = \mu_a \int_S d\vec{r} \int_{2\pi} I(\vec{r}, \hat{s}) d\hat{s} = \mu_a \sum_{i=1}^N \int_{S_i} d\vec{r} \int_{2\pi} I_i(\vec{r}, \hat{s}) d\hat{s}. \quad (18)$$

Using the expression of the radiance in 2D obtained in the previous section, we have as follows:

$$P_A = \mu_a \sum_{i=1}^N \int_{S_i} d\vec{r} \int_{2\pi} I_i(\vec{r}, \hat{s}) d\hat{s} = 2\pi I_e \sum_{i=1}^N S_i \left(\frac{n_i}{n_e} \right), \quad (19)$$

and, then,

$$\langle L \rangle = \pi \frac{\sum_{i=1}^N S_i \left(\frac{n_i}{n_e} \right)}{P}. \quad (20)$$

Thus, the invariance property remains valid also in inhomogeneous media with variations of refractive index. The above demonstration also holds in the presence of “cavities.” In the following, we show the results of numerical computations in some cases, and we compare them with the analytical formula of Eqs. (16) and (20).

III. NUMERICAL SIMULATIONS

We simulated light diffusion by generating a large number of random walkers and letting them propagate in the sample volume. We do not take into account interference effects because, due to the stochastic character of the diffusion process, phase information can be neglected.

The numerical simulations in the 3D case are based on a well-tested Monte Carlo (MC) code, developed during the 1990s [40–42]. The robustness of the core of the code, i.e., the generation of trajectories, is checked to be in excellent agreement with exact analytical expressions [43]. Each step of length ℓ of a trajectory is randomly drawn by the exponential probability density function,

$$p(\ell) = \mu_s \exp(-\mu_s \ell). \quad (21)$$

Given a uniformly distributed random number $\xi \in [0, 1]$, each step of the random walk is obtained by the usual inversion of the cumulative distribution associated with Eq. (21),

$$\ell(\xi) = -\mu_s^{-1} \ln(1 - \xi). \quad (22)$$

The used scattering function is the Henyey-Greenstein [44], here, considered with $g = 0$.

The isotropic uniform illumination condition has been implemented by reproducing a Lambertian distribution of the entrance angles, that is a distribution that follows the cosine law. A crossover of an interface between two different media is considered as a new scattering event in terms of step length extraction, whereas the change in direction is deterministically established by Snell's law.

Also the radiance I and the fluence Φ (the integral over the solid angle of the radiance I) have been calculated, considering the external surface of the medium as illuminated by a unitary input flux of 1 W/m^2 (see the Appendix).

Then, within a generic subvolume V_i of the medium, the radiance is constant and equal to

$$I_i = \frac{1}{\pi} (n_i/n_e)^2 \text{ W/m}^2 \text{ sr}. \quad (23)$$

The corresponding fluence is as follows:

$$\Phi_i = 4\pi I_i = 4(n_i/n_e)^2 \text{ W/m}^2. \quad (24)$$

An independent MC code has been used for the 2D case, considering the same expression [Eq. (22)] for the generation of the length between two scattering events. Its robustness has been then tested with the analytical results for the IP in the condition of the absence of refractive-index mismatches.

In Fig. 2, a simulated trajectory is shown, considering a 2D circular medium with a circular decentered inhomogeneity with different refractive indices and scattering coefficients. Also, a refractive-index mismatch is present between the external environment and the largest medium.

IV. RESULTS

In all the results shown in this paper, the label ‘‘SIM’’ is referred to the data generated by MC simulations, whereas the label IP is referred to values obtained by the theory.

TABLE I. Retractive index of the i th layer of the media used in the reported 3D simulations. The layer 0 is the external environment (see Fig. 3). In media D and E the refractive index varies linearly in the 100 layers between the two extreme values by an increment of 0.01.

		Layer index i				
		0	1	2	3	4
A	n_i	1.00	2.00	1.00	2.00	1.00
B	n_i	2.00	1.00	2.00	1.00	2.00
C	n_i	1.00	1.25	1.50	1.75	2.00
		Layer index i				
		0	1,2,...,100			
D	n_i	1.00	1.01,1.02,...,2.00			
E	n_i	2.00	1.99,1.98,...,1.00			

A. The 3D case

In Fig. 3, the structure of a medium simulated in the 3D case is shown. A sphere composed of four layers, characterized by a refractive-index n_i and a scattering coefficient μ_i , is immersed in an external environment with a refractive-index n_0 . The radiation impinges upon the external layer from the outside uniformly and isotropically. Five different cases, characterized by different parameters, are labeled with the letters A – E and described in Table I (superscript in the plot legend). The external environment is labeled as Layer 0. The radius of the sphere is 5 mm and, in cases A – C , the second, the third, and the fourth layers have radius 4, 3, and 2 mm, respectively. The cases D and E are characterized by 100 layers with a refractive index that becomes larger or smaller as the depth d from the outermost layer increases.

For the same μ_s in the whole medium, each MC calculation consists of 100 independent simulations of 10^8 (case A – C) or 10^7 (case D and E) independent trajectories in order to evaluate the standard error of the averaged mean path-length $\langle L \rangle_{\text{SIM}}$.

Figure 4 shows $\langle L \rangle_{\text{SIM}}$ as a function of μ_s for the media A – C . In these cases, the strong refractive-index mismatch between two adjacent layers leads to a relatively high reflection at the interface. In the figure, the values predicted by the generalized IP [Eq. (16)] are also reported. The results show that the mean path length of the random walkers is consistent with the value predicted by theory over five orders of magnitude of the scattering coefficient μ_s .

Figures 5 and 6 show the results for the media composed by 100 layers with a refractive index that linearly increases or decreases as the layer index i grows (see Table I), or, equivalently, as the distance d from the surface increases. In these figures, the fluence as a function of d and the profile of the radiance for three values of d are also shown. The fluence has a constant value within each layer and increasing or decreasing values as the layer change. The radiance, within the noise of the MC simulations, shows a constant angular profile as expected where the IP holds.

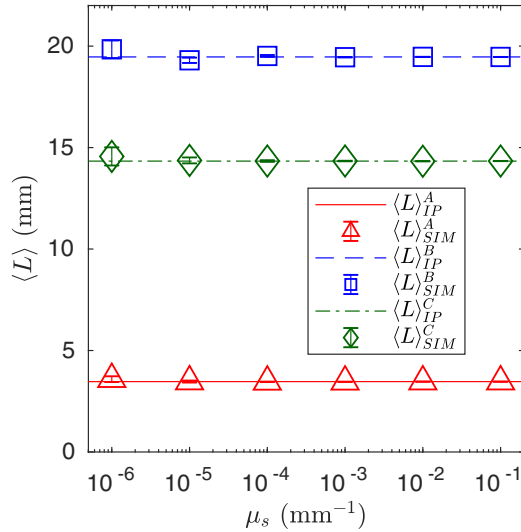


FIG. 4. The 3D case: $\langle L \rangle$ for different values of μ_s for the media A–C (see Table I). The markers are referred to MC simulations, and the lines are referred to the values expected by IP.

B. The 2D case

In the simulations of the 2D case, we analyze the cases of homogeneous and nonhomogeneous media. As shown in Fig. 2, a typical medium consists of a circle immersed in an external environment and with an inhomogeneity inside. Such an inhomogeneity is a circle with a different refractive index and scattering coefficient and has a center located at a random

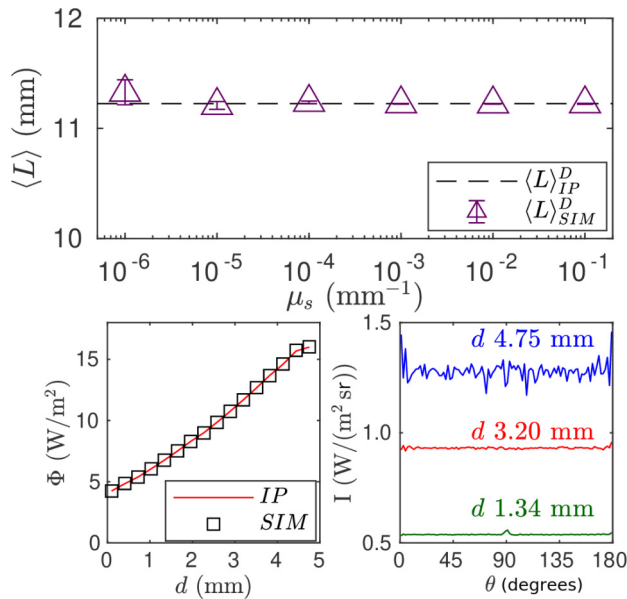


FIG. 5. The 3D case: On the top, $\langle L \rangle$ for different values of μ_s for the medium D (see Table I). The markers are referred to MC simulations, and the lines to the values are expected by IP. For the case of $\mu_s = 10^{-1} \text{ mm}^{-1}$, on the bottom left and on the bottom right, the fluence (the markers are MC data, and the lines are IP values) as a function of the depth d from the surface of the largest sphere and the radiance data of MC simulations for three depths are reported, respectively.

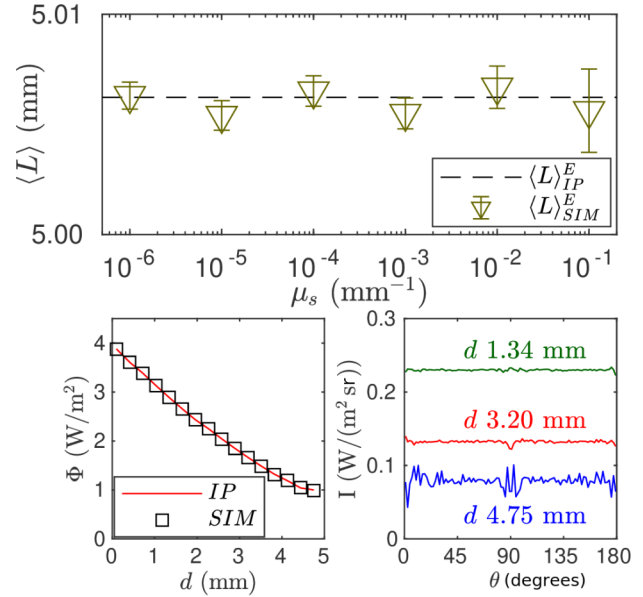


FIG. 6. The 3D case: On the top, the mean path-length $\langle L \rangle$ for different values of μ_s for the medium E (see Table I). The markers are referred to MC simulations, and the lines are referred to the values expected by IP. For the case of $\mu_s = 10^{-1} \text{ mm}^{-1}$, on the bottom left and on the bottom right, the fluence (the markers are MC data, and the lines are IP values) as a function of the depth d from the surface of the largest sphere and the radiance data of MC simulations for three depths are reported, respectively.

position respect to the center of the larger circle. Each result, for a fixed set of parameters, consists of ten independent simulations of 2×10^8 trajectories.

In Fig. 7 (top left), the mean path-length $\langle L \rangle$ for different values of the radius R_2 of the circular decentered inhomogeneity is shown. The largest medium has radius $R_1 = 1 \text{ mm}$. The refractive indices of the external environment (n_0), the largest medium (n_1), and the inhomogeneity (n_2) are 1, 2, and 1, respectively. The scattering coefficient is 0.5 mm^{-1} everywhere.

Figure 7 (top right) shows $\langle L \rangle$ for different values of the refractive index n_1 of the largest medium. The refractive index is 1 in the external environment and in the decentered inhomogeneity. The radii of the largest medium and of the inhomogeneity are $R_1 = 1$ and $R_2 = 0.5 \text{ mm}$, respectively. The scattering coefficient is everywhere constant (0.5 mm^{-1}).

In Fig. 7 (bottom), the refractive index of the external environment (n_0) and of the decentered inhomogeneity n_2 are 1, whereas n_1 is 2. The radii of the largest medium and of the inhomogeneity is $R_1 = 1$ and $R_2 = 0.4 \text{ mm}$, respectively, whereas the scattering coefficient of the inhomogeneity is 1 mm^{-1} . In this case, $\langle L \rangle$ is shown as a function of the scattering coefficient μ_1 of the largest medium.

In all the 2D cases analyzed, the MC results for $\langle L \rangle$ (red markers) are consistent within the standard error (of an order of 10^{-3} – 10^{-4}) with the value predicted by Eq. (20) (solid blue line).

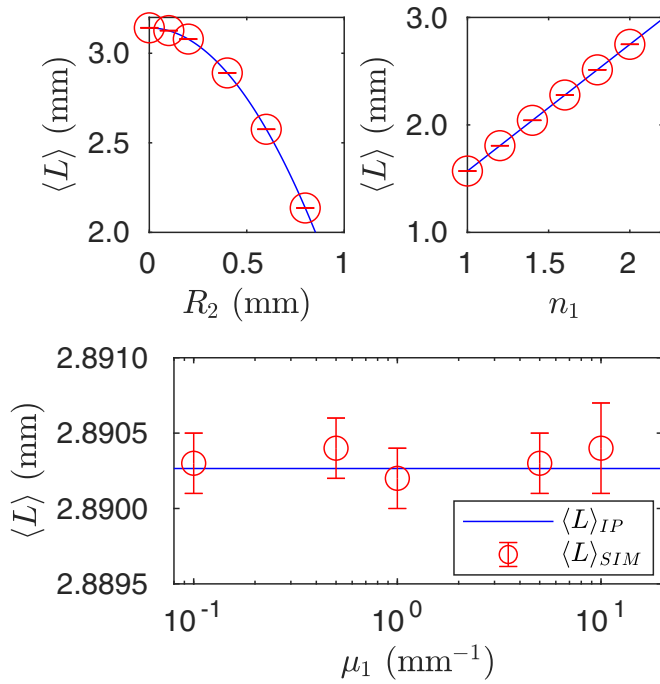


FIG. 7. The 2D case: $\langle L \rangle$ for different values of the radius R_2 of the circular decentered inhomogeneity (top-left figure), $\langle L \rangle$ as a function of the refractive index n_1 (top-right figure) and $\langle L \rangle$ for different values of the scattering coefficient μ_1 of the largest medium (bottom figure). (The markers are MC data, and the lines are IP values.)

V. CONCLUSIONS

The mean path-length invariance property has been investigated in the case of light diffusion in the presence of refractive-index mismatch between a medium and the external environment as well as for inhomogeneous media. Analytical results are found both for the two-dimensional and the three-dimensional cases. Numerical calculations are in full agreement with analytical expressions.

Thus, in the paper, the invariance property is shown to remain valid for all classes of inhomogeneous media with discrete variations of refractive index in their internal domain. This is a further generalization of this property that also opens the possibility to use its prediction to a quite larger class

of problems. This fact can be exploited to obtain reference values for photon migration studies in random media. For instance, the IP represents a unique and powerful tool able to validate any MC code extensively used to simulate random walk processes with an arbitrary precision.

From the point of view of practical applications in tissue optics and photovoltaics, such a paper helps to understand the optical propagation in the most general kind of medium, i.e., an inhomogeneous material with scattering and refractive-index mismatches.

ACKNOWLEDGMENTS

Acknowledgments are due to Prof. G. Zaccanti for his help in performing the MC simulations.

APPENDIX: TOTAL INPUT FLUX

The shown results for the radiance and the fluence are referred to an external surface illuminated by a uniform isotropic illumination for the radiance (Lambertian illumination) with the further hypothesis to have a unitary total input flux in the medium, given by the integral of the radiance over the whole solid semiangle [45]. This fact implies that only the normal component of \vec{J}_{in} is not null. Given I_{in} as the input radiance, we have that

$$J_{\text{in}} = \int_{2\pi} I_{\text{in}} \hat{s} \cdot \hat{n} d\hat{s} = \pi I_{\text{in}}, \quad (\text{A1})$$

and, then,

$$I_{\text{in}} = \frac{1 \text{ W/m}^2}{\pi}. \quad (\text{A2})$$

The corresponding input fluence is as follows:

$$\Phi_{\text{in}} = \int_{2\pi} I_{\text{in}} d\hat{s} = 2 \text{ W/m}^2. \quad (\text{A3})$$

In a generic subvolume, the radiance is as follows:

$$I_i = \left(\frac{n_i}{n_e} \right)^2 I_{\text{in}}, \quad (\text{A4})$$

and the fluence,

$$\Phi_i = 4\pi I_i. \quad (\text{A5})$$

-
- [1] S. L. Jacques, *Phys. Med. Biol.* **58**, R37 (2013).
 [2] T. Durduran, R. Choe, W. B. Baker, and A. G. Yodh, *Rep. Prog. Phys.* **73**, 076701 (2010).
 [3] D. R. Leff, O. J. Warren, L. C. Enfield, A. Gibson, T. Athanasiou, D. K. Patten, J. Hebden, G. Z. Yang, and A. Darzi, *Breast Cancer Res. Treat.* **108**, 9 (2008).
 [4] G. Zaccanti, S. D. Bianco, and F. Martelli, *Appl. Opt.* **42**, 4023 (2003).
 [5] D. S. Wiersma, *Nat. Phys.* **4**, 359 (2008).
 [6] N. M. Lawandy, R. M. Balachandran, A. S. L. Gomes, and E. Suvain, *Nature (London)* **368**, 436 (1995).
 [7] E. Ignesti, F. Tommasi, L. Fini, S. Lepri, V. Radhakrishmi, D. S. Wiersma, and S. Cavalieri, *Phys. Rev. A* **88**, 033820 (2013).
 [8] F. Tommasi, E. Ignesti, L. Fini, and S. Cavalieri, *Phys. Rev. A* **91**, 033820 (2015).
 [9] F. Tommasi, L. Fini, E. Ignesti, S. Lepri, F. Martelli, and S. Cavalieri, *Phys. Rev. A* **98**, 053816 (2018).
 [10] M. Segev, Y. Silberberg, and D. N. Christodoulides, *Nat. Photonics* **7**, 197 (2013).
 [11] H. Cao, J. Y. Xu, D. Z. Zhang, S. H. Chang, S. T. Ho, E. W. Seelig, X. Liu, and R. P. H. Chang, *Phys. Rev. Lett.* **84**, 5584 (2000).
 [12] P. Barthelemy, J. Bertolotti, and D. S. Wiersma, *Nature (London)* **453**, 495 (2008).
 [13] J. Bertolotti, K. Vynck, and D. S. Wiersma, *Phys. Rev. Lett.* **105**, 163902 (2010).

- [14] F. Tommasi, L. Fini, F. Martelli, and S. Cavalieri, *Phys. Rev. A* **99**, 063836 (2019).
- [15] N. Gofraniha, I. Viola, F. Di Maria, G. Barbarella, G. Gigli, L. Leuzzi, and C. Conti, *Nat. Commun.* **6**, 6058 (2015).
- [16] A. S. L. Gomes, E. P. Raposo, A. L. Moura, S. I. Fewo, P. I. R. Pincheira, V. Jerez, L. J. Q. Maia, and C. B. d. Araújo, *Sci. Rep.* **6**, 27987 (2016).
- [17] F. Tommasi, E. Ignesti, S. Lepri, and S. Cavalieri, *Sci. Rep.* **6**, 37113 (2016).
- [18] R. C. Polson and Z. V. Vardeny, *Appl. Phys. Lett.* **85**, 1289 (2004).
- [19] P. Di Ninni, F. Martelli, and G. Zaccanti, *Phys. Med. Biol.* **56**, N21 (2011).
- [20] E. Ignesti, F. Tommasi, L. Fini, F. Martelli, N. Azzali, and S. Cavalieri, *Sci. Rep.* **6**, 35225 (2016).
- [21] G. Vasquez, Y. Hernández, and Y. Coello, *Sci. Rep.* **8**, 14903 (2018).
- [22] F. Tommasi, E. Ignesti, L. Fini, F. Martelli, and S. Cavalieri, *Opt. Express* **26**, 27615 (2018).
- [23] H. A. Atwater and A. Polman, *Nature Mater.* **9**, 205 (2010).
- [24] M. A. Green and S. Pillai, *Nat. Photonics* **6**, 130 (2012).
- [25] R. Mupparapu, K. Vynck, T. Svensson, M. Burrese, and D. S. Wiersma, *Opt. Express* **23**, A1472 (2015).
- [26] F. Pratesi, M. Burrese, F. Riboli, K. Vynck, and D. S. Wiersma, *Opt. Express* **21**, A460 (2013).
- [27] F. Bigourdan, R. Pierrat, and R. Carminati, *Opt. Express* **27**, 8666 (2019).
- [28] F. Tommasi, L. Fini, F. Martelli, and S. Cavalieri, *Opt. Commun.* **458**, 124786 (2020).
- [29] S. Blanco and R. Fournier, *Europhys. Lett.* **61**, 168 (2003).
- [30] J. Bardsley and A. Dubi, *SIAM J. Appl. Math.* **40**, 71 (1981).
- [31] R. Pierrat, P. Ambichl, S. Gigan, A. Haber, R. Carminati, and S. Rotter, *Proc. Natl. Acad. Sci. USA* **111**, 17765 (2014).
- [32] P. A. M. Dirac, British Report MS-D-5, Part I (1943).
- [33] R. Savo, R. Pierrat, U. Najar, R. Carminati, S. Rotter, and S. Gigan, *Science* **358**, 765 (2017).
- [34] G. Frangipane, G. Vizsnyiczai, C. Maggi, R. Savo, A. Sciortino, S. Gigan, and R. Di Leonardo, *Nat. Commun.* **10**, 2442 (2019).
- [35] A. Mazzolo, *Europhys. Lett.* **68**, 350 (2004).
- [36] A. Zoia, C. Larmier, and D. Mancusi, *Europhys. Lett.* **127**, 20006 (2019).
- [37] A. Zoia, E. Dumonteil, and A. Mazzolo, *Europhys. Lett.* **100**, 40002 (2012).
- [38] C. de Mulatier, A. Mazzolo, and A. Zoia, *Europhys. Lett.* **107**, 30001 (2014).
- [39] F. Jenkins and H. White, *Fundamentals of Optics*, 4th ed. (McGraw-Hill, New York, 1976).
- [40] G. Zaccanti, *Appl. Opt.* **30**, 2031 (1991).
- [41] D. Contini, F. Martelli, and G. Zaccanti, *Appl. Opt.* **36**, 4587 (1997).
- [42] A. Sassaroli, C. Blumetti, F. Martelli, L. Alianelli, D. Contini, A. Ismaelli, and G. Zaccanti, *Appl. Opt.* **37**, 7392 (1998).
- [43] G. Zaccanti, E. Battistelli, P. Brusaglioni, and Q. N. Wei, *Pure Appl. Opt.* **3**, 897 (1994).
- [44] L. G. Henyey and J. L. Greenstein, *Astrophys. J.* **93**, 70 (1941).
- [45] F. Martelli, S. Del Bianco, A. Ismaelli, and G. Zaccanti, *Light Propagation through Biological Tissue and Other Diffusive Media: Theory, Solutions, and Software* (SPIE, Bellingham, WA, 2009).